Inorganic Chemistry
Article

Inorg. Chem. **2011**, *50*, 245–249 **245**
DOI: 10.1021/ic101925a

Crystal Structures, Electronic Structures, and Physical Properties of Tl_4MQ_4 (M = Zr or Hf; Q = S or Se)

Cheriyedath Raj Sankar, Savitree Bangarigadu-Sanasy, Abdeljalil Assoud, and Holger Kleinke*

Department of Chemistry, University of Waterloo, Waterloo, ON, Canada N2L 3G1

Received September 20, 2010

The ternary thallium chalcogenides of the general formula Tl_4MQ_4 (M = Zr or Hf; Q = S or Se) were obtained from high-temperature reactions without air. These sulfides and selenides are isostructural, crystallizing in the triclinic system with space group $P\bar{1}$ and $Z = 5$, in contrast to Tl_4MTe_4 compounds that adopt space group $R\bar{3}$. The unit cell parameters for Tl_4ZrS_4 are as follows: a = 9.0370(5) Å, b = 9.0375(5) Å, c = 15.4946(9) Å, α = 103.871(1)°, β = 105.028(1)°, γ = 90.138(1)°, and V = 1183.7(1) Å^3. In contrast to the corresponding tellurides, the sulfides and selenides exhibit edge-shared MQ_6 octahedra, propagating along the c axis in a zigzag manner. All elements occur in the most common oxidation states, according to the formulation $(Tl^{+})_4M^{4+}(Q^{2-})_4$. Electronic structure calculations predict energy band gaps of 1.7 eV for Tl_4ZrS_4 and 1.3 eV for Tl_4ZrSe_4, which are in accordance with the large resistivity values observed experimentally.

Introduction

Heavy metal chalcogenides have attracted an increasing level of attention because of their promising thermoelectric properties.[1−4] Some of the well-known Tl-based thermoelectrics are Tl_9AgTe_5 (figure of merit ZT = 1.2 at 700 K),[5] Tl_9BiTe_6 (ZT = 1.2 at 500 K),[6] $TlSbTe_2$ (ZT = 0.87 at 715 K),[7] Tl_4SnTe_3 (ZT = 0.74 at 673 K),[8] and Tl_4PbTe_3 (ZT = 0.71 at 673 K).[8]

Recently, we began to explore some thallium-rich chalcogenides that contain group 4 metal atoms such as Zr and Hf. Our first result was the discovery of two new thallium−group 4−telluride compounds, Tl_4MTe_4 (M = Zr and Hf) that comprise triple units of face-condensed MTe_6 distorted octahedra.[9] Several ternary thallium or alkali metal chalcogenides of such 4-1-4 formulas, with group 4 or group 14 elements, have been identified.[10−15] Na_4SnS_4 and Na_4SnSe_4 are isostructural (space group $P\bar{4}2_1c$), whereas K_4SnSe_4 (*Pnma*) is different[11] and in turn isostructural with Na_4SiSe_4.[16] Na_4TiSe_4 adopts another different structure in space group $I2/a$.[10] All of these $A_4M'Q_4$ compounds (A = Na or K; M′ = Si, Ge, Sn, or Ti) are composed of isolated tetrahedral anionic $[M'Q_4]^{4-}$ units. Some Tl-based chalcogenides of the series $Tl_4M'Q_4$ (M′ = Ti, Si, Ge, or Sn; Q = S or Se) are also known to exist.[13−15] Tl_4TiQ_4 and Tl_4SnQ_4 crystallize in the monoclinic crystal system with space group $P2_1/c$;[13] Tl_4SiS_4 and Tl_4GeS_4 are reported to adopt space group Cc,[14,15] and Tl_4SiSe_4 is reported to adopt space group $C2/c$.[14] This $Tl_4M'Q_4$ series also shares the $[M'Q_4]^{4-}$ units mentioned above that are separated by Tl atoms. In all these cases, weakly bonding Tl−Tl contacts are between 3.4 and 4.0 Å in length. Some of these ternary thallium−group 4−chalcogenide compounds show interesting thermoelectric properties as well.[9,17]

There have been few reports about the structure and properties of the Zr or Hf counterparts of the chalcogenides mentioned above. Phase diagram studies of the Tl_2Q-ZrQ_2 (Q = S, Se, or Te) systems[18] pointed toward the existence of Tl_4ZrS_4 and Tl_4ZrSe_4, but not Tl_4ZrTe_4, while no such studies

*To whom correspondence should be addressed. E-mail: kleinke@uwaterloo.ca.

(1) Rowe, D. M. *Thermoelectrics Handbook: Macro to Nano*; CRC Press, Taylor & Francis Group: Boca Raton, FL, 2006.
(2) Snyder, G. J.; Toberer, E. S. *Nat. Mater.* **2008**, *7*, 105–114.
(3) Sootsman, J. R.; Chung, D. Y.; Kanatzidis, M. G. *Angew. Chem., Int. Ed.* **2009**, *48*, 8616–8639.
(4) Kleinke, H. *Chem. Mater.* **2010**, *22*, 604–611.
(5) Kurosaki, K.; Kosuga, A.; Muta, H.; Uno, M.; Yamanaka, S. *Appl. Phys. Lett.* **2005**, *87*, 061919/1–061919/3.
(6) Wölfing, B.; Kloc, C.; Teubner, J.; Bucher, E. *Phys. Rev. Lett.* **2001**, *86*, 4350–4353.
(7) Kurosaki, K.; Uneda, H.; Muta, H.; Yamanaka, S. *J. Alloys Compd.* **2004**, *376*, 43–48.
(8) Kosuga, A.; Kurosaki, K.; Muta, H.; Yamanaka, S. *J. Appl. Phys.* **2006**, *99*, 063705.
(9) Sankar, C. R.; Bangarigadu-Sanasy, S.; Assoud, A.; Kleinke, H. *J. Mater. Chem.* **2010**, *20*, 7485–7490.
(10) Klepp, K. O. *Z. Naturforsch., B: Chem. Sci.* **2000**, *55*, 39–44.
(11) Klepp, K. O. *Z. Naturforsch., B: Chem. Sci.* **1992**, *47*, 411–417.
(12) Klepp, K. O. *Z. Naturforsch., B: Chem. Sci.* **1985**, *40*, 878–882.
(13) Klepp, K. O.; Eulenberger, G. *Z. Naturforsch., B: Chem. Sci.* **1984**, *39*, 705–712.
(14) Eulenberger, G. *Acta Crystallogr.* **1986**, *C42*, 528–534.
(15) Eulenberger, G. *Z. Kristallogr.* **1977**, *145*, 427–436.
(16) Preishuber-Pflugl, H.; Klepp, K. O. *Z. Kristallogr.—New Cryst. Struct.* **2003**, *218*, 383–384.
(17) Sabov, M. Y.; Sevryukov, D. V.; Galagovets, I. V.; Betsa, V. V.; Peresh, E. Y. *Inorg. Mater.* **2010**, *46*, 11–13.
(18) Sabov, M. Y.; Peresh, E. Y.; Barchii, I. E. *Ukr. Khim. Zh.* (*Russ. Ed.*) **1998**, *64*, 18–21.

Published on Web 12/08/2010

Table 1. Crystallographic Data of Tl_4MQ_4

formula	Tl_4ZrS_4	Tl_4HfS_4	Tl_4ZrSe_4	Tl_4HfSe_4
formula weight (g/mol)	1036.94	1124.21	1224.54	1311.81
T of measurement (K)	296(2)	296(2)	296(2)	296(2)
wavelength (Å)	0.71073	0.71073	0.71073	0.71073
crystal system	triclinic	triclinic	triclinic	triclinic
space group	$P\bar{1}$	$P\bar{1}$	$P\bar{1}$	$P\bar{1}$
a (Å)	9.0370(5)	9.032(1)	9.274(2)	9.288(8)
b (Å)	9.0375(5)	9.035(1)	9.264(2)	9.271(8)
c (Å)	15.4946(9)	15.448(2)	16.007(3)	16.01(1)
α (deg)	103.871(1)	103.768(2)	104.146(3)	104.11(1)
β (deg)	105.028(1)	104.759(2)	105.326(3)	105.05(1)
γ (deg)	90.138(1)	90.125(2)	90.219(3)	90.09(1)
V (Å^3)	1183.7(1)	1181.2(2)	1282.7(5)	1288(2)
Z	5	5	5	5
ρ_{calcd} (g/cm^3)	7.273	7.902	7.926	8.458
no. of collected, unique, observed reflections (R_{int})	16813, 6867, 5377 (0.056)	9118, 6337, 4970 (0.033)	12888, 7296, 4460 (0.045)	9280, 6715, 3304 (0.074)
R1/wR2 [$I > 2\sigma(I)$][a]	0.042/0.089	0.065/0.139	0.068/0.111	0.108/0.236

[a] $R1 = \sum||F_o| - |F_c||/\sum|F_o|$; $wR2 = \{\sum[w(F_o^2 - F_c^2)^2]/\sum[w(F_o^2)^2]\}^{1/2}$.

on the Hf counterparts were performed to the best of our knowledge. With this contribution, we present the crystal structures, electronic structures, and electrical resistance of Tl_4ZrS_4, Tl_4HfS_4, Tl_4ZrSe_4, and Tl_4HfSe_4.

Experimental Section

Syntheses and Analyses. The target compositions were synthesized from the constituent elements stored in an argon-filled glovebox [Tl granules, 99.9% (Alfa Aesar); Zr powder, 325 mesh, 98.5% (including 2% Hf) (Alfa Aesar); Hf powder, 100 mesh, 99.8% (including 1% Zr) (Alfa Aesar); and Te chunks, 99.9% (Aldrich)]. The elements were loaded in the required stoichiometry into glassy carbon crucibles, which were then introduced into silica ampules and sealed under vacuum. These ampules were heated slowly to 1073 K in a resistance furnace, allowed to remain at 1073 K for 100 h, and finally slowly cooled to room temperature. To analyze the phase purity, we measured the powder X-ray patterns of the samples using an Inel powder diffractometer with a position-sensitive detector and Cu Kα_1 radiation. In case of the sulfides, all reflections belonged to the title compounds, Tl_4MS_4, while minor unidentified reflections were present in the case of the selenides in addition to those of the target compounds. The samples exhibited no noticeable reaction under ambient conditions in air.

The glassy carbon crucibles are not required for the formation of Tl_4MQ_4, but their presence prevents tube attack; the first reactions without these crucibles yielded high but not 100% yields of all four Tl_4MQ_4 chalcogenides, while the samples were sticking to the silica walls. This method led to the formation of $Tl_6Si_2Te_6$ as a very minor side product during attempts to prepare Tl_4ZrTe_4.

Energy dispersive X-ray analysis (EDAX) using the LEO 1530 electron microscope with an additional EDAX device, EDAX Pegasus 1200, revealed the presence of the three elements, Tl, M, and Q, approximately in the expected 4:1:4 ratio.

The thermal behavior of these materials was studied via differential scanning calorimetry using the Netzsch STA 409PC Luxx instrument in an argon atmosphere as described previously.[19] Both sulfides melt congruently around 1000 K (Tl_4ZrS_4) and 984 K (Tl_4HfS_4), whereas the selenides melt incongruently around 797 K (both Tl_4ZrSe_4 and Tl_4HfSe_4). The latter explains the presence of minor side products as well as the poor crystal quality in the case of the selenides. These results are in qualitative agreement with the work on the Tl_2Q-ZrQ_2 phase diagrams mentioned above,[18] wherein the respective melting and/or decomposition points were determined to be 985 K for Tl_4ZrS_4 and 805 K for Tl_4ZrSe_4.

Single-Crystal Structure Determinations. Suitable single crystals (rectangular blocks or plates) were picked from the respective bulk sample for the single-crystal X-ray diffraction analysis. The data were collected at room temperature using a Bruker Smart Apex CCD diffractometer that employs Mo Kα radiation, by scans of 0.3° in ω at three different φ angles with exposure times of 30 s each for a total of 3 × 600 frames in each case. The data were treated for Lorentz and polarization corrections. The absorption corrections were based on fitting a function to the empirical transmission surface as sampled by multiple equivalent measurements. The APEX II package,[20] which includes SAINT[21] and SHELXTL,[22] was used for the data reduction and structure refinement.

The single-crystal X-ray diffraction analysis of the crystal picked from the Tl_4ZrS_4 batch showed that the compound crystallizes in the triclinic system, with space group $P\bar{1}$. After the successful structure solution and refinement, we tentatively refined the occupancies of the Tl atom sites, although the thermal expansion parameters were inconspicuous. The lowest Tl site occupancy [Tl3, 0.985(3)] was equal to full occupancy within 5 times its standard deviation. Next, we fixed all Tl occupancies at 1.0 and refined the Zr occupancies, resulting in values between 1.000(4) and 1.014(3). Hence, all occupancies were kept at 1.0 in the final refinement. Finally, ADDSYMM was used to check for any missed symmetry, and the atomic positions were standardized with TIDY within the PLATON package.[23] The highest remaining peak of the electron density synthesis of 3.3 e/Å^3 was located only 0.8 Å from Tl7, and the deepest hole of −4.4 e/Å^3 was 0.8 Å from Tl4.

Single crystals of Tl_4HfS_4, Tl_4ZrSe_4, and Tl_4HfSe_4 were also analyzed, and all of them (while of a poorer quality because of their incongruent melting and small crystal sizes) were found to be isostructural with Tl_4ZrS_4. The crystallographic data of all four compounds are listed in Table 1, and the atomic positions and equivalent displacement parameters of Tl_4ZrS_4 are listed in Table 2.

Electronic Structure Calculations and Electrical Resistivity Measurements. The electronic structure calculations were performed using the self-consistent tight binding first-principles linear muffin-tin orbital (LMTO) method that uses the atomic

(19) Assoud, A.; Soheilnia, N.; Kleinke, H. *Chem. Mater.* **2005**, *17*, 2255–2261.

(20) *M86-Exx078 APEX2 User Manual*; Bruker AXS Inc.: Madison, WI, 2006.

(21) Sheldrick, G. M. *Acta Crystallogr.* **2008**, *A64*, 112–122.

(22) Sheldrick, G. M. *SHELXTL*, version 5.12; Siemens Analytical X-Ray Systems: Madison, WI, 1995.

(23) Spek, A. L. *J. Appl. Crystallogr.* **2003**, *36*, 7–13.

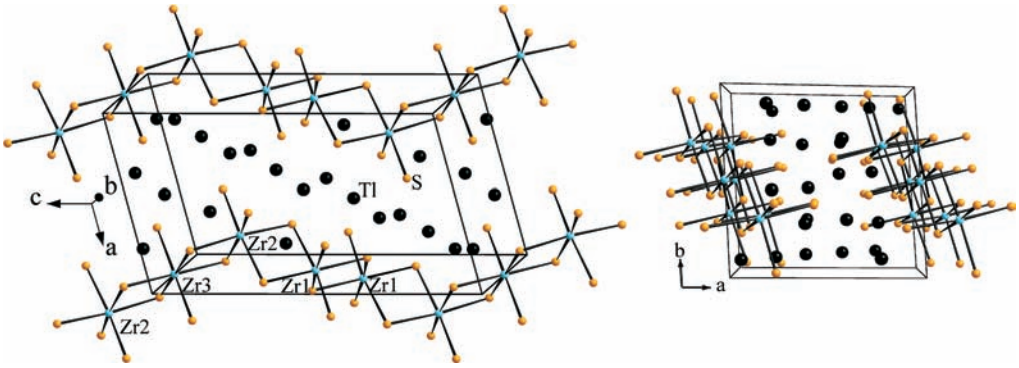

Figure 1. Crystal structure of Tl_4ZrS_4 viewed along the *b* (left) and *c* (right) axes. Tl−S bonds have been omitted for the sake of clarity.

Table 2. Atomic Positions and Equivalent Displacement Parameters[a] of Tl_4ZrS_4

atom	site	*x*	*y*	*z*	U_{eq} (Å^2)
Tl1	2*i*	0.05058(5)	0.08212(5)	0.80084(3)	0.0230(1)
Tl2	2*i*	0.22063(5)	0.72301(5)	0.40061(3)	0.0230(1)
Tl3	2*i*	0.22368(5)	0.08791(5)	0.59828(3)	0.0240(1)
Tl4	2*i*	0.22668(5)	0.44869(5)	0.79582(3)	0.0222(1)
Tl5	2*i*	0.37987(5)	0.09446(5)	0.39232(3)	0.0247(1)
Tl6	2*i*	0.39207(5)	0.70404(5)	0.19360(3)	0.0243(1)
Tl7	2*i*	0.41442(5)	0.46169(5)	0.59957(3)	0.0238(1)
Tl8	2*i*	0.58003(5)	0.09753(5)	0.19975(3)	0.0237(1)
Tl9	2*i*	0.60692(5)	0.72061(5)	0.00129(3)	0.0231(1)
Tl10	2*i*	0.77123(5)	0.09999(5)	0.00683(3)	0.0233(1)
Zr1	2*i*	0.0175(1)	0.6827(1)	0.59971(6)	0.0114(2)
Zr2	2*i*	0.1745(1)	0.3075(1)	0.19931(6)	0.0116(2)
Zr3	1*c*	0	0.5	0	0.0122(3)
S1	2*i*	0.0600(3)	0.0497(3)	0.4033(2)	0.0164(5)
S2	2*i*	0.0679(3)	0.3937(3)	0.5789(2)	0.0133(5)
S3	2*i*	0.0704(3)	0.2308(3)	0.0201(2)	0.0124(5)
S4	2*i*	0.0889(3)	0.5818(3)	0.1792(2)	0.0134(5)
S5	2*i*	0.2386(3)	0.0352(3)	0.1955(2)	0.0162(5)
S6	2*i*	0.2525(3)	0.3861(3)	0.3783(2)	0.0140(5)
S7	2*i*	0.4431(3)	0.3784(3)	0.1962(2)	0.0166(5)
S8	2*i*	0.7098(3)	0.2484(3)	0.3958(2)	0.0158(5)
S9	2*i*	0.7257(3)	0.4292(3)	0.0025(2)	0.0168(5)
S10	2*i*	0.9022(3)	0.2635(3)	0.2223(2)	0.0131(5)

[a] U_{eq} is defined as one-third of the trace of the orthogonalized U_{ij} tensor.

Table 3. Selected Interatomic Interactions of Tl_4ZrS_4

	CN	distance range (Å)	PBO[a]	valence sum[b]
Tl1−S	5	2.837(3)−3.297(2)	0.58	0.47
Tl2−S	5	2.931(2)−3.289(3)	0.54	0.39
Tl3−S	4	2.838(3)−3.147(2)	0.59	0.51
Tl4−S	5	2.897(3)−3.325(3)	0.59	0.45
Tl5−S	4	2.901(3)−3.270(3)	0.59	0.49
Tl6−S	4	2.885(3)−3.299(3)	0.60	0.52
Tl7−S	5	2.846(3)−3.261(2)	0.55	0.42
Tl8−S	4	2.833(3)−3.170(3)	0.59	0.51
Tl9−S	4	2.849(3)−3.275(3)	0.59	0.51
Tl10−S	5	2.886(2)−3.300(3)	0.55	0.40
Zr1−S	6	2.520(3)−2.642(3)	4.32	2.17
Zr2−S	6	2.520(3)−2.664(3)	4.20	2.08
Zr3−S	6	2.571(3)−2.600(2)	4.16	2.01

[a] Cumulated Pauling bond order. [b] Total bond-valence sum.

spheres approximation (ASA).[24,25] In this method, the density functional theory (DFT) is employed, which utilizes the local density approximation (LDA) for the exchange and correlation energies. The following wave functions were used: 6s, 6p, 6d, and 5f for Tl (the latter two downfolded[26]); 5s, 5p, 4d, and 4f for Zr (4f downfolded); 3s, 3p, and 3d for S (3d downfolded); and 4s, 4p, and 4d for Se (4d downfolded). The eigenvalue problems were solved on the basis of 132 *k* points selected with an improved tetrahedron method[27] within the irreproducible wedge of the first Brillouin zone. The electrical resistivity measurements were performed using a standard four-probe method, employing a Keithley 2400 source/measure unit.

Crystal Structure. The title compounds are isostructural. Here we focus on Tl_4ZrS_4 as their representative. Its structure contains three crystallographically distinct Zr atoms, which are octahedrally (distorted) coordinated by S atoms. These ZrS_6 octahedra are edge-shared to form a zigzag chain running along the *c* axis (left part of Figure 1). Therein, the metal atom sequence is −Zr2−Zr3−Zr2−Zr1−Zr1−. The edge-shared octahedra form triple units, in which the Zr atoms (Zr2−Zr3−Zr2) are arranged in a linear fashion (the angle being 180°). Two such units are connected by a dimeric edge-shared unit of $Zr1S_6$ octahedra, with a Zr3−Zr2−Zr1 angle of 122°.

These chains are separated from each other by the Tl atoms along the *a* and *b* axes (right part of Figure 1). The Zr−S bond lengths vary from 2.52 to 2.66 Å (Table 3), which are within the normal range of Zr−S distances as in ZrS_2 of 2.57 Å.[28] The corresponding Zr−Se bonds are significantly longer because of the larger atomic radius of Se, and the Hf−Q bonds are generally slightly shorter than the corresponding Zr−Q bonds because of the slightly smaller atomic radius of Hf, compared to that of Zr.

The Zr−Zr distances within the chains of Tl_4ZrS_4 are 3.82 Å (Zr2−Zr3), 3.92 Å (Zr3−Zr1), and 3.89 Å (Zr1−Zr1) and thus too long for significant interactions. The same is true for the S−S distances, which are all greater than 3.4 Å. Therefore, standard formal charges according to $(Tl^+)_4Zr^{4+}(S^{2-})_4$ can be assumed.

The Tl−S distances range from 2.83 to 3.30 Å in Tl_4ZrS_4, comparable with those in $Tl_4M'Q_4$ (M′ = Ti, Si, or Sn) of 2.90−3.45 Å.[13,14] Of the 10 crystallographically independent Tl sites, five (Tl1, Tl2, Tl4, Tl7, and Tl10) are connected to five S atoms and the remaining five to four S atoms each. Moreover, numerous Tl−Tl contacts as short as 3.69 Å exist. The coordination spheres around all Tl atoms are severely distorted because of the lone pair effect (filled 6s orbital) of Tl^+ (Figure 2).

To look for systematic differences between the 4- and 5-fold coordinated Tl atoms, we performed bond-valence sum calculations according to the work of Pauling[29] and Brese and

(24) Andersen, O. K. *Phys. Rev. B* **1975**, *12*, 3060–3083.
(25) Hedin, L.; Lundqvist, B. I. *J. Phys. C* **1971**, *4*, 2064–2083.
(26) Lambrecht, W. R. L.; Andersen, O. K. *Phys. Rev. B* **1986**, *34*, 2439–2449.
(27) Blöchl, P. E.; Jepsen, O.; Andersen, O. K. *Phys. Rev. B* **1994**, *49*, 16223–16233.
(28) McTaggart, F. K.; Wadsley, A. D. *Aust. J. Chem.* **1958**, *11*, 445–457.
(29) Pauling, L. *The Nature of the Chemical Bond*, 3rd ed.; Cornell University Press: Ithaca, NY, 1948.

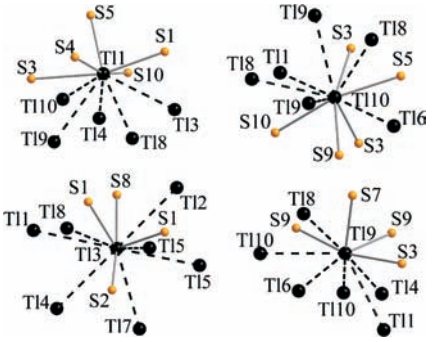

Figure 2. Selected Tl coordination spheres of Tl_4ZrS_4.

Figure 3. Tl atom network in the structure of Tl_4ZrS_4. Zr and S atoms have been omitted for the sake of clarity.

O'Keeffe.[30] The Pauling bond orders, PBO_{ij}, were calculated for each bond via the relationship $PBO_{ij} = \exp[(R_{ij}^{P} - d_{ij})/0.6\ Å]$ and the bond valences, v_{ij}, via the relationship $v_{ij} = \exp[(R_{ij} - d_{ij})/0.37\ Å]$, where d_{ij} is the distance between the two selected atoms, R_{ij}^{P} is the sum of their single-bond Pauling radii, and R_{ij} is empirically derived from a comparison of known sulfides to be 2.63 Å for Tl−S bonds and 2.41 Å for Zr−S bonds.[30] When $r_{Tl} = 1.44$ Å, $r_{Zr} = 1.45$ Å, and $r_S = 1.04$ Å, we obtain an R_{ij}^{P} values of 2.48 Å for Tl−S bonds and 2.49 Å for Zr−S bonds.[29] Then, the PBO_{ij} and v_{ij} values were summed to obtain total bond orders and valence sums, respectively, as listed in Table 3 for Tl_4ZrS_4. In all cases, the cumulated Pauling bond orders were higher than the bond-valence sums, the latter being much smaller than expected, between 0.39 and 0.52 for the Tl atoms and between 2.01 and 2.17 for the Zr atoms. For the latter, the PBOs (4.16−4.32) are quite consistent and close to the expected value of 4. The PBOs of the Tl atoms are smaller than expected, and the 4-fold coordinated atoms appear to have slightly higher values (0.59−0.60) than the 5-fold ones (0.54−0.59). The same trend occurs in the valence sums (0.49−0.52 vs 0.39−0.47).

The Tl−Tl contacts with distances ranging from 3.69 to 3.99 Å may be considered to be weak interactions when compared to the strong Tl−Tl bonding in elemental Tl and weak interactions in Tl tellurides such as Tl_5Te_3,[31] Tl_4ZrTe_4,[9] and $Tl_6Si_2Te_6$:[32] the elemental (hexagonal) Tl has two different Tl−Tl distances of 3.41 and 3.46 Å, while these tellurides exhibit Tl−Tl interactions ranging from 3.49 to 4.03 Å in length. These weak Tl−Tl interactions of Tl_4ZrS_4 result in chains of Tl atoms containing octahedra, cubes, and less regular rhomboids. These chains, running along the *b* axis, are interconnected via Tl7−Tl7 contacts of 3.99 Å to puckered slabs parallel to the *b*−*c* plane (Figure 3).

While Tl_4ZrS_4 and Tl_4ZrSe_4 are isostructural, Tl_4ZrTe_4 adopts a unique structure type.[9] Therein, $ZrTe_6$ octahedra are face-condensed unlike the edge-condensed ZrQ_6 octahedra in Tl_4ZrS_4 and Tl_4ZrSe_4, allowed by the larger size of the Te atoms compared to S and Se. A common feature of all these chalcogenides is the occurrence of a multitude of weak Tl−Tl contacts, resulting in a three-dimensional network of Tl atoms.

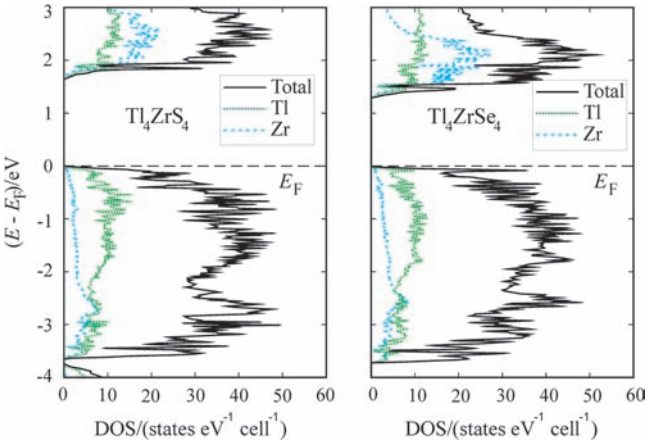

Figure 4. Densities of states for Tl_4ZrS_4 (left) and Tl_4ZrSe_4 (right).

Electronic Structure Calculations and Electrical Resistivity Measurements. The densities of states (DOS) curves for Tl_4ZrS_4 and Tl_4ZrSe_4 are shown in Figure 4. Both materials appear to be semiconductors. The valence bands are extended over 3.5 eV and dominated by the S and Se p states, respectively. The Tl 6s states are located below these valence bands. The Tl and Zr contributions to the valence band are consequences of covalent mixing with the Q p states. The largest contributions to the conduction bands arise from the Zr 4d states.

The calculated band gap of Tl_4ZrS_4 of 1.7 eV is in agreement with the high resistivity (on the order of 10^7 Ω cm at room temperature) of the sample. The corresponding selenide has a smaller calculated band gap of 1.3 eV (room temperature resistivity of 10^5 Ω cm). The colors observed for both sulfides (dark red, corresponding to a gap of ∼1.9 eV) and both selenides (black, corresponding to a gap of < 1.7 eV) also confirm the trend of the decreasing gap size from the sulfides to the selenides, noting that DFT calculations typically underestimate the gap size. Lastly, the stoichiometric tellurides, Tl_4ZrTe_4 and Tl_4HfTe_4, were predicted to be narrow band gap semiconductors, with a band gap of approximately 0.3 eV, and determined to have room-temperature resistivity values of < 0.4 Ω cm.[9]

The integrated crystal orbital Hamilton populations, ICOHPs,[33,34] confirm that the Tl−Tl contacts are bonding as postulated before. For example, the ICOHP value of the Tl2−Tl5 bond with its 3.69 Å length is −0.11 eV, and the longer Tl7−Tl7 bond of 3.99 Å also has a significant, albeit small, ICOHP of −0.04 eV, indicative of a minor net bonding character. For comparison, the bonds in elemental Tl of 3.41 and 3.46 Å exhibit ICOHP values of −0.48 and −0.42 eV, respectively. Thus, the ICOHP value of the shortest Tl−Tl interaction in Tl_4ZrS_4 amounts to 24% of the ICOHP average of the bonds of the element, confirming the weak but significant bonding character.

Conclusions

Room-temperature single-crystal X-ray diffraction results revealed that the four chalcogenides of the formula Tl_4MQ_4 (M = Zr or Hf; Q = S or Se) are isostructural, crystallizing in a new structure type. A zigzag chain of edge-sharing MQ_6 octahedra and an infinite network of Tl atoms occur in these chalcogenides.

(30) Brese, N. E.; O'Keeffe, M. *Acta Crystallogr.* **1991**, *B47*, 192–197.
(31) Schewe, I.; Böttcher, P.; von Schnering, H. G. *Z. Kristallogr.* **1989**, *188*, 287–298.
(32) Assoud, A.; Soheilnia, N.; Kleinke, H. *J. Solid State Chem.* **2006**, *179*, 2707–2713.
(33) Dronskowski, R.; Blöchl, P. E. *J. Phys. Chem.* **1993**, *97*, 8617–8624.
(34) Landrum, G. A.; Dronskowski, R. *Angew. Chem., Int. Ed.* **2000**, *39*, 1560–1585.

With no Q−Q bonds present, all elements adopt their most common oxidation states, namely, Tl^{+}, M^{4+}, and Q^{2-}. These materials are shown by calculation to be intrinsic semiconductors, supported by their dark red appearance in the case of the sulfides and the measured high room-temperature resistivity values in all cases. Thus, they cannot be used as thermoelectric materials. The corresponding tellurides exhibit an entirely different structure with face-sharing MTe_6 octahedra and much smaller band gaps, resulting in promising thermoelectric properties as described previously.[9]

Acknowledgment. Acknowledgment is made to the Natural Sciences and Engineering Research Council of Canada for financial support of this research. H.K. is furthermore indebted to the Natural Sciences and Engineering Research Council of Canada for the Canada Research Chair award.

Supporting Information Available: Four crystallographic information files (CIF). This material is available free of charge via the Internet at http://pubs.acs.org.